

Multi-Frequency Sparse Array-Based Massive MIMO Radar for Autonomous Driving

Shunqiao Sun¹ and Yimin D. Zhang²

¹ Department of Electrical and Computer Engineering, The University of Alabama, Tuscaloosa, AL, USA

² Department of Electrical and Computer Engineering, Temple University, Philadelphia, PA, USA

E-mail: shunqiao.sun@ua.edu, ydzhang@temple.edu

Abstract—In this paper, we propose the concept of high-resolution massive multiple-input multiple-output (MIMO) radar with large-aperture sparse arrays for autonomous driving by exploiting multi-frequency signaling. The diversity offered by multi-frequency signals renders a high number of virtual sensors that effectively increase the degrees of freedom. Two strategies are developed to synthesize virtual sparse arrays by jointly utilizing MIMO radar sum coarray and multi-frequency signaling, respectively with and without further incorporating the difference coarray concept. As an example, we synthesize sparse arrays with an aperture of around 100 normalized half-wavelength using only 7 physical array elements in the context of the proposed multi-frequency MIMO radar.

Index Terms—automotive radar, autonomous driving, multi-frequency sparse arrays, matrix completion, MIMO radar

I. INTRODUCTION

Automotive radars have found increasingly important in advanced driver assistance systems, such as adaptive cruise control and automatic emergency braking. According to studies conducted by the National Highway Traffic Safety Administration (NHTSA), 37,461 Americans died on U.S. highways in 2016 as a result of automobile accidents [1], of which 94% were due to human errors [2]. To remedy this problem, radar has emerged as one of the key technologies in autonomous driving systems. Some of today's self-driving vehicles, such as Zoox, are equipped with more than 10 radars, providing a 360° surround sensing capability under all weather conditions [3–5]. Automotive radar is the largest commercial market for radar outside of defense. Automotive radars are typically operated in millimeter-wave frequencies between 76–81 GHz [5, 6]. Other frequency bands, such as 120–260 GHz, are also possible for automotive radar applications [7–9].

Unlike conventional surveillance radars, automotive radars are typically operated for a short range (within multi-hundred meters) and must meet strict requirements on their size (multi-inch by multi-inch), power (multi-watt), and cost. They are required to be integrated behind the vehicle bumper or windshield and operated in a highly dynamic propagation environment with rich multipath [5].

Existing automotive multiple-input multiple-output (MIMO) radar transceivers, such as Texas Instruments (TI) AWR1243, typically support 3 transmit and 4 receive antennas [10], rendering a total number of 12 sum coarray elements to achieve angular resolution of around 10 degrees. Level 4/Level 5 autonomous driving requires higher angular resolution to generate *point clouds* which represent the shapes of surrounding objects [11, 12] and enable target identification using deep neural network-based machine learning techniques [13, 14].

Automotive radars achieve high spatial resolution using antenna arrays with a large array aperture. When using a conventional uniform linear array (ULA) with half-wavelength interelement spacing, the aperture is proportional to the number of array sensors. As such,

high-resolution target direction-of-arrival (DOA) estimation requires a high number of antennas which are often infeasible in automotive radar applications due to the strict cost constraints. One of the effective techniques to enable cost reduction of automotive radars is MIMO radar [15]. MIMO radar technologies have been commonly exploited by most major suppliers in different types of automotive radar products, including short-range, medium-range, and long-range radars [11, 16–18].

The cost of synthesizing a large virtual ULA with half-wavelength interelement spacing in the context of MIMO radar technology is still high for mass production of automotive radars. One way to further reduce the cost without sacrificing the angular resolution is to exploit nonuniform or sparse linear arrays (SLAs), in lieu of ULAs, for MIMO radar synthesis [19, 20]. MIMO radar systems exploiting SLA configurations reduce the required number of transmit and receive antennas by removing a subset of antenna sensors from a ULA with half-wavelength interelement spacing. As such, the effective interelement spacing of the corresponding virtual array becomes larger than half wavelength, while the array aperture remains the same as that of the original ULA based on which the SLA is obtained. A number of sparse array configurations, such as the minimum redundant array (MRA) [21], nested array [22], coprime array [23, 24], and maximum interelement spacing constraint (MISC) array [25], have been reported in the literature.

SLAs using the difference coarray concept provide a scheme to estimate a high number of targets that may exceed the number of array elements. However, obtaining difference coarrays requires a high number of data snapshots that enable accurate array covariance matrix estimation. In highly dynamic automotive scenarios, however, it is often challenging to collect target data over multiple coherent processing intervals because the positions of both radar-mounted vehicle and objects may change rapidly [5]. As a result, only few snapshots or even a single snapshot are available for DOA estimation [26]. Interpolation and extrapolation techniques are attractive to automotive radars by filling missing holes in the synthesized SLA [27, 28].

In this paper, we propose a novel sparse array framework that utilizes multi-frequency signals to enable higher spatial degrees of freedom (DOFs) for high-resolution DOA estimation. Signal processing techniques are developed to achieve effective DOA estimation for various array configurations with uniform or irregular virtual sensor locations.

The concept of constructing virtual arrays by exploiting two or more frequencies was first developed for coprime arrays using a single ULA [29, 30], and was recently extended to general sparse array designs [31, 32]. In this paper, we deal with multi-frequency sparse arrays in the context of MIMO radar for automotive applications.

II. MIMO RADAR WAVEFORM DESIGN

A. FMCW Radar

Frequency-modulated continuous-wave (FMCW) waveforms are commonly used in existing automotive radars because they enable high-resolution target range and velocity estimation while requiring low-cost samplers at the receivers [5]. An FMCW waveform is a periodical linear frequency modulated signal, also known as a chirp signal, that is transmitted with a certain pulse repetition frequency. At the receiver, the target echo signal is correlated with the transmitted chirp, yielding a complex sinusoidal *beat signal*. The narrow bandwidth of the beat signal is a major reason to use FMCW signals in automotive radar because the beat signal can be digitized using a low-speed analog-to-digital converter (ADC) at a low cost.

The frequency of the beat signal is associated with the target range information, whereas the phase variation of the beat signal over slow-time pulses renders the Doppler frequency of the targets. As such, the targets are first separated in the range and Doppler domains. As a result, the number of targets in the same range-Doppler bin is typically small, thereby facilitating DOA estimation with sparse sensing techniques based on compressive sensing [33, 34]. Recently, phase-modulated continuous-wave (PMCW) radars are also considered in automotive radars that offer better waveform orthogonality but require higher receiver complexity [5].

B. MIMO Radar Waveform Design with Dual Frequencies

Consider an automotive radar equipped with M_t transmit and M_r receive antennas. Each transmit antenna transmits a sequence of N FMCW chirps that sweep at two carrier frequencies, f_1 and f_2 , respectively, with the same sweep bandwidth of B . At each receiver, the echo signals are mixed with transmitted chirps respectively at the two carrier frequencies to obtain beat signals. To achieve waveform orthogonality, the chirps are multiplied with a phase code that is different for each antenna and changes for each chirp. We denote such phase code as $x_m(n) = e^{j2\pi\alpha_m(n)}$ for $m = 1, \dots, M_t$ and $n = 1, \dots, N$. The phase codes are designed such that the Doppler fast Fourier transform (FFT) of the interference can be distributed into the entire Doppler spectrum as pseudo noise. One of such phase codes is Chu sequences [35].

III. MULTI-FREQUENCY SPARSE MIMO RADARS

In this section, we consider two ways to exploit multi-frequency sparse MIMO radars based on the number of available array snapshots. The first one utilizes the difference coarray concept whereas the second does not. In the proposed multi-frequency sparse MIMO radar, the array snapshot is referred to as the array response at a particular time instance consisting of data obtained at all virtual receivers and corresponding to the same range-Doppler bin.

A. Multi-Frequency Sparse MIMO Radar Exploiting Difference Coarray Concept

We extend the array synthesis approach for sparse arrays [29] to MIMO radars. We consider a two-frequency case, and the locations of the transmit and receive antennas are designed such that the synthesized sum coarrays corresponding to the two carrier frequencies, f_1 and f_2 , form ULAs with interelement spacing of $M_1\lambda_1/2$ and $M_2\lambda_2/2$, respectively. Here, M_1 and M_2 are coprime integers, $f_2 = (M_2/M_1)f_1$, and λ_1 and λ_2 are the respective wavelengths corresponding to these two frequencies. Such sum coarrays can be achieved, for example, using physical transmit and receive antenna arrays that are ULAs with interelement spacing of $M_1\lambda_1/2$ and

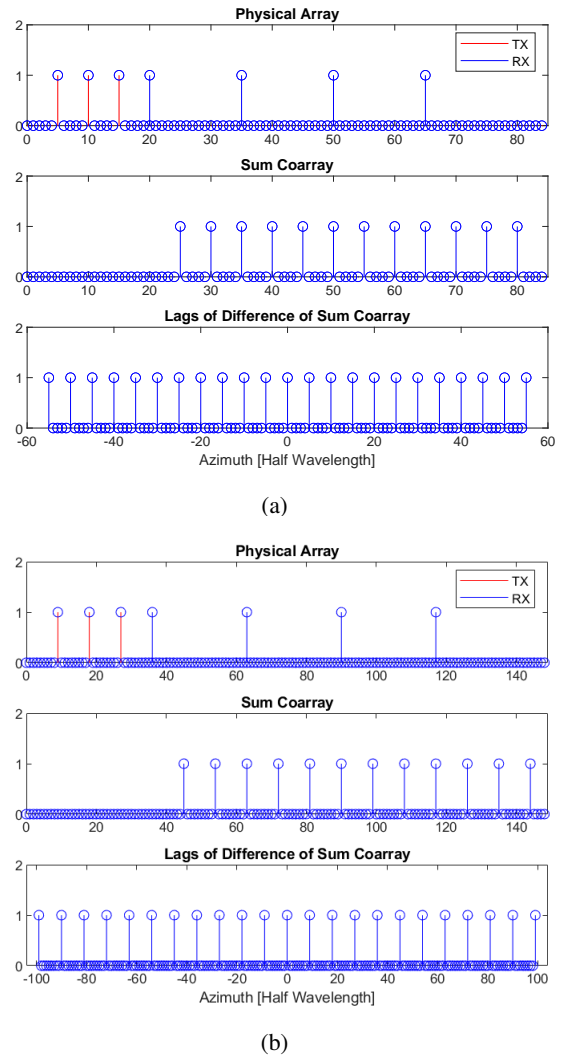


Fig. 1. The physical array, sum coarray, and lags of difference coarray of sum coarray: (a) at frequency f_1 ; (b) at frequency f_2 .

$M_t M_1 \lambda_1 / 2$, respectively [36]. The virtual sensor set of the resulting sum coarray can be expressed as

$$\mathbb{S} = \{M_1 n_1 d_0, 0 \leq n_1 \leq M_t M_r - 1\} \cup \{M_2 n_2 d_0, 0 \leq n_2 \leq M_t M_r - 1\}, \quad (1)$$

where d_0 denotes half-wavelength in a normalized frequency. When an adequate number of snapshots are available to construct the array covariance matrix, a difference coarray can be constructed by utilizing the difference lags of this sum coarray.

As an illustrative example for multi-frequency sparse MIMO radar exploiting difference coarrays, we consider a radar transceiver consisting of $M_t = 3$ transmit and $M_r = 4$ receive antennas. The physical transmit and receive antennas are located at $[1, 2, 3] M_1 d$ and $[4, 7, 10, 13] M_1 d$, respectively, where $M_1 = 5$, $M_2 = 9$, and $d = \lambda_1 / 2$. We choose $f_1 = 78$ GHz and $f_2 = (M_2 / M_1) f_1 = 140.4$ GHz. In this case, two virtual ULAs corresponding to the two carrier frequencies are synthesized with coprime element spacings, as shown in Fig. 1.

The two sum coarrays corresponding to the two carrier frequencies are combined together such that the reference element is at position

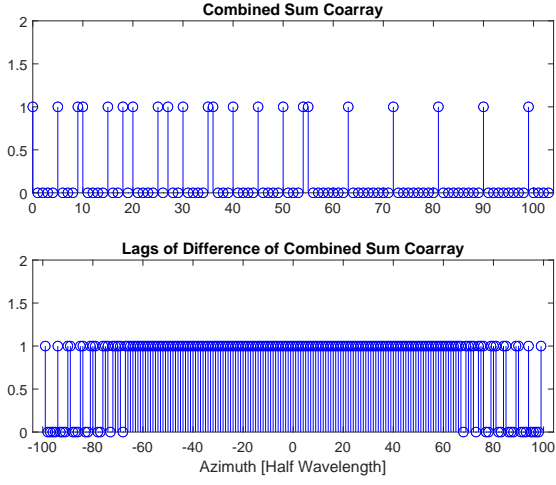


Fig. 2. The sum of combined coarray and the corresponding difference lags of the combined sum coarray.

zero. The difference coarray of the combined sum coarray is shown in Fig. 2. It can be found that the difference lags of the combined sum coarray has 135 successive lags on the half-wavelength grid. There are holes which can be filled using, e.g., matrix completion approaches [31, 37, 38].

B. Multi-Frequency Sparse MIMO Radar without Exploiting Difference Coarray Concept

In highly dynamic scenarios as commonly encountered in autonomous driving, the number of array snapshots is limited. As a result, it may not be able to utilize difference coarray as its applicability relies on an adequate number of data snapshots to reconstruct an accurate array covariance matrix. In this case, instead of synthesizing a large difference coarray with consecutive lag positions, one useful strategy is to design a dual-frequency sparse MIMO radar with randomly deployed transmit and receive array antennas to synthesize a random sum coarray.

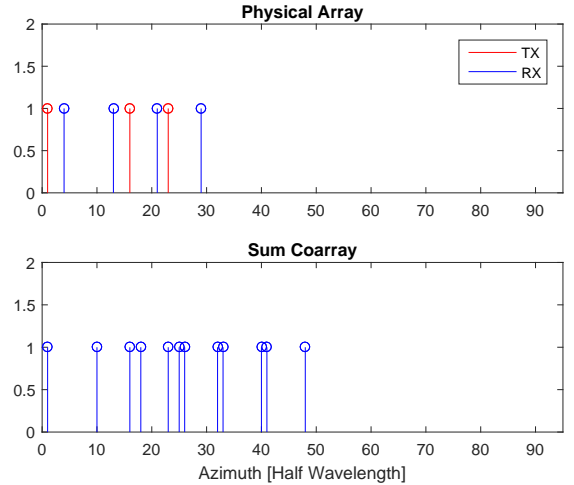
In Fig. 3, we give an example of two-frequency sparse MIMO radar. As shown in Fig. 3(a), the physical transmit and receive antennas are located at [1, 16, 23] $\lambda_1/2$ and [4, 13, 21, 29] $\lambda_1/2$, respectively. When assuming $f_2 = 2f_1$, the sum coarrays obtained for the two frequencies are shown in Figs. 3(a) and 3(b). These sum coarrays can be combined together.

IV. DOA ESTIMATION USING MULTI-FREQUENCY SPARSE MIMO RADAR

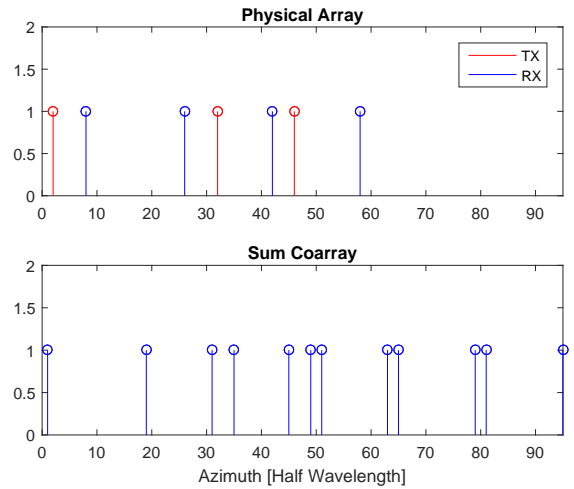
Consider K targets with their respective DOAs denoted as θ_k , $k = 1, \dots, K$. The sparse array with Q_1 virtual antennas are located over a grid with a total number of Q_2 grid points and the grid size is normalized to half wavelength. In the absence of noise, the SLA response is expressed as

$$\mathbf{y}_S = \mathbf{A}_S \mathbf{s} \in \mathbb{C}^{Q_1 \times 1}, \quad (2)$$

where $\mathbf{A}_S = [\mathbf{a}_S(\theta_1), \dots, \mathbf{a}_S(\theta_K)]$ is the array manifold matrix with the associated steering vector expressed as $\mathbf{a}_S(\theta_k) = [1, e^{j\frac{2\pi}{\lambda}d_1 \sin(\theta_k)}, \dots, e^{j\frac{2\pi}{\lambda}d_{Q_1-1} \sin(\theta_k)}]^T$, and d_i is the position of the i -th element of SLA with respect to the reference element. Here, λ is the normalized wavelength. In addition, $\mathbf{s} = [\beta_1, \dots, \beta_K]^T$,



(a)



(b)

Fig. 3. Physical array and sum coarray for dual-frequency MIMO sparse array: (a) carrier frequency f_1 ; (b) carrier frequency $f_2 = 2f_1$.

where β_k denotes the amplitude associated with the k -th target. With the sparse array response \mathbf{y}_S , we can construct a vector $\mathbf{y} \in \mathbb{C}^{Q_2 \times 1}$ of which $Q_2 - Q_1$ elements are zeros, corresponding to the locations where no virtual antennas are placed.

In general, there are two directions to carry out the DOA estimation in multi-frequency sparse arrays, depending on whether the holes of sparse array are filled or not.

A. DOA Estimation with Array Interpolation

It is noted that, because the random sum coarray formed from the multi-frequency sparse MIMO radar is sparse, it is vital to deal with the high sidelobe levels by filling the holes in the combined random sum coarray via matrix completion [38].

Denote $N_2 = \lfloor Q_2/2 \rfloor$ and $N_1 = Q_2 - N_2 \geq N_2$, where $\lfloor \cdot \rfloor$ denotes the floor function. Then, we can formulate $\mathbf{y} \in \mathbb{C}^{Q_2 \times 1}$ into N_2 overlapped subarrays of length N_1 . Based on those subarrays, we formulate a Hankel matrix $\mathbf{X} \in \mathbb{C}^{N_1 \times N_2}$ with its (i, j) -th element given as $\mathbf{X}_{ij} = \mathbf{y}_{i+j-1}$ for $i = 1, \dots, N_1$ and $j = 1, \dots, N_2$. Matrix \mathbf{X} has many missing entries and thus can be viewed as a thinned version of the corresponding matrix \mathbf{Y} constructed from

the virtual ULA with half wavelength spacing. Under certain mild conditions, the missing elements can be fully recovered by solving a relaxed nuclear norm optimization problem conditioned on the observed entries, expressed as [39]

$$\min \|\mathbf{X}\|_* \quad \text{s.t.} \quad \mathbf{X}_{ij} = \mathbf{Y}_{ij}, \quad (i, j) \in \Omega, \quad (3)$$

where $\|\cdot\|_*$ denotes the nuclear norm of a matrix, and Ω is the set of indices of the observed entries that is determined by the SLA configuration. Once matrix \mathbf{Y} is recovered, the full array response is obtained by averaging its anti-diagonal entries.

Fig. 4(a) shows the beampattern of the two-frequency sparse MIMO radar with sum coarray example given in Fig. 3. It can be found that the sidelobe of the sparse array is relatively high without filling the holes or optimally choosing the virtual sparse array element locations. Fig. 4(b) compares the FFT spectra of the sparse array response with holes as well as that for the filled full array after performing matrix completion, where the input signal-to-noise ratio (SNR) is set to 20 dB. Two targets are located at DOAs of 10° and 20° , respectively. It can be found that the sidelobe levels are substantially lowered when the holes of a sparse array are filled via matrix completion. DOAs can be estimated via standard array processing methods based on the array response corresponding to the completed matrix \mathbf{Y} .

In the multi-frequency sparse MIMO radar exploiting the difference coarray, we can also synthesize a virtual array with large consecutive ULA or carry out virtual array interpolation to fill the holes [37, 38]. As a result, the DOA estimation can be implemented via the commonly used subspace-based methods, such as MUSIC and ESPRIT. DOA estimation can also be carried out using compressive sensing by exploiting the group sparsity of the signals across different frequencies [31].

B. DOA Estimation without Array Interpolation

For multi-frequency sparse MIMO radar without exploiting difference coarrays, target DOA estimation can be based on digital beamforming or compressive sensing, provided that the peak sidelobe levels (PSLs) of the sparse array are controlled to be sufficiently low.

When performing compressive sensing-based DOA estimation, we need to discretize the DOA space into N fine grids, and the K targets are assumed to be on the grid. The array response can be written as

$$\mathbf{y} = \mathbf{A}\boldsymbol{\beta} + \mathbf{n}, \quad (4)$$

where $\mathbf{A} = [\mathbf{a}(\theta_1), \dots, \mathbf{a}(\theta_N)]$ is the basis matrix and $\boldsymbol{\beta} = [\beta_1, \dots, \beta_N]$ is a sparse vector with K non-zero elements. The target DOAs can be found by solving an ℓ_1 norm optimization problem, such as the Dantzig selector [40] defined as

$$\begin{aligned} \min \quad & \|\boldsymbol{\beta}\|_{\ell_1} \\ \text{s.t.} \quad & \left\| \mathbf{A}^H (\mathbf{y} - \mathbf{A}\boldsymbol{\beta}) \right\|_{\ell_\infty} < \eta, \end{aligned} \quad (5)$$

or greedy methods, such as orthogonal matching pursuit (OMP) [41].

The coherence of the sensing matrix used in compressive sensing, defined as

$$\mu \triangleq \max_{i \neq l} \frac{|\mathbf{a}^H(\theta_i) \mathbf{a}(\theta_l)|}{\|\mathbf{a}(\theta_i)\|_{\ell_2} \|\mathbf{a}(\theta_l)\|_{\ell_2}}, \quad (6)$$

needs to be kept low in order to obtain uniform recovery guarantees [42]. In the above expression, $\mathbf{a}(\theta_i)$ is the steering vector of the SLA at direction θ_i . It can be easily verified that the value of μ is the PSL of the array beampattern [43]. Therefore, it is vital to design multi-frequency sparse MIMO radars with a low PSL.

V. CONCLUSIONS

In this paper, we proposed a cost-effective massive MIMO radar system for autonomous driving by exploiting both multi-frequency signaling and sparse MIMO radar concepts. The proposed radar systems have been shown to significantly increase the degrees of freedom in virtual array aperture to enable high-resolution target DOA estimation for autonomous driving. Two strategies to synthesize a virtual sparse array have been developed. DOA estimation with and without incorporating array interpolation were examined for the proposed multi-frequency sparse MIMO radar.

REFERENCES

- [1] U.S. Department of Transportation's National Highway Traffic Safety Administration (NHTSA), "2016 fatal motor vehicle crashes: Overview," [Available Online] <https://www.nhtsa.gov/press-releases/usdot-releases-2016-fatal-traffic-crash-data>, Oct. 6, 2017.
- [2] L. Ecola, S. W. Popper, R. Silbergliitt, and L. Fraade-Blanar, "The road to prepared for a vision for achieving zero roadway deaths by 2050," RAND Corporation Report, [Available Online] https://www.rand.org/pubs/research_reports/RR2333.html, April 18, 2018.
- [3] S. Patole, M. Torlak, D. Wang, and M. Ali, "Automotive radars: A review of signal processing techniques," *IEEE Signal Process. Mag.*, vol. 34, no. 2, pp. 22–35, 2017.
- [4] F. Engels, P. Heidenreich, A. M. Zoubir, F. Jondral, and M. Wintermantel, "Advances in automotive radar: A framework on computationally efficient high-resolution frequency estimation," *IEEE Signal Process. Mag.*, vol. 34, no. 2, pp. 36–46, 2017.
- [5] S. Sun, A. P. Petropulu, and H. V. Poor, "MIMO radar for advanced driver-assistance systems and autonomous driving: Advantages and challenges," *IEEE Signal Process. Mag.*, vol. 37, no. 4, pp. 98–117, 2020.
- [6] J. Hasch *et al.*, "Millimeter-wave technology for automotive radar sensors in the 77 GHz frequency band," *IEEE Trans. Microw. Theory Tech.*, vol. 60, no. 3, pp. 845–860, 2012.
- [7] European Telecommunications Standards Institute (ETSI), "System reference document (SRdoc); short range devices (SRD) using ultra wide band (UWB); transmission characteristics; technical characteristics for SRD equipment using ultra wide band technology (UWB); radiodetermination application within the frequency range 120 GHz to 260 GHz," *ETSI Tech. Rep. 103 498 V1.1.1 (2019-02)*, 2019.
- [8] A. Banerjee *et al.*, "Millimeter-wave transceivers for wireless communication, radar, and sensing," in *Proc. IEEE Custom Integrated Circuits Conf.*, Austin, TX, April 2019.
- [9] A. Visweswaran *et al.*, "A 145GHz FMCW-radar transceiver in 28nm CMOS," in *Proc. IEEE Int. Solid-State Circuits Conf.*, San Francisco, CA, Feb. 2019.
- [10] Texas Instruments, "AWR1243 single-chip 77- and 79-GHz FMCW transceiver," datasheet, 2017.
- [11] I. Bilik *et al.*, "Automotive MIMO radar for urban environments," in *Proc. IEEE Radar Conf.*, Philadelphia, PA, May 2016.
- [12] F. Meinel, M. Stolz, M. Kunert, and H. Blume, "An experimental high performance radar system for highly automated driving," in *Proc. Int. Conf. Microwaves for Intelligent Mobility (ICMIM)*, Nagoya, Japan, Mar. 2017.
- [13] C. R. Qi, H. Su, K. Mo, and L. J. Guibas, "PointNet: Deep learning on point sets for 3D classification and segmentation," in *Proc. IEEE Conf. Computer Vision and Pattern Recognition (CVPR)*, Honolulu, HI, July 2017.
- [14] C. R. Qi, L. Yi, H. Su, and L. J. Guibas, "PointNet++: Deep hierarchical feature learning on point sets in a metric space," in *Proc. Conf. Neural Information Processing Systems (NIPS)*, Long Beach, CA, Dec. 2017.
- [15] J. Li and P. Stoica, "MIMO radar with colocated antennas," *IEEE Signal Process. Mag.*, vol. 24, no. 5, pp. 106–114, 2007.
- [16] S. Alland and J. Searcy, "Radar system and method of digital beamforming," U.S. Patent 2009/0085800, April 2, 2009.
- [17] M. Wintermantel, "Radar system with improved angle formation," U.S. Patent 2011/0074621, Mar. 31, 2011.
- [18] M. Schoor *et al.*, "Method for operating a MIMO radar," U.S. Patent 2014/0347211, Nov. 27, 2014.

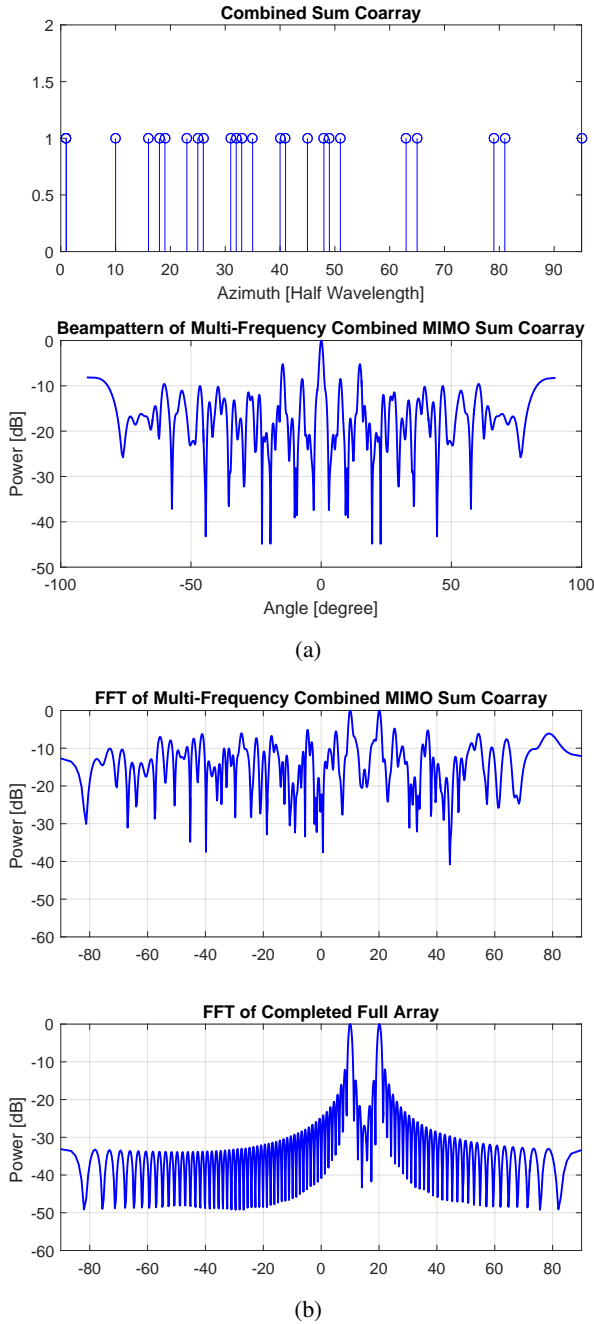


Fig. 4. Combined sum coarray and array beampatterns. (a) Combined sum coarray from dual-frequency and its array beampattern; (b) The FFT beampattern of combine sum coarray and completed full array corresponding to two targets at 10° and 20° , $\text{SNR} = 20\text{dB}$.

[19] C. Schmid, R. Feger, C. Wagner, and A. Stelzer, "Design of a linear non-uniform antenna array for a 77-GHz MIMO FMCW radar," in *Proc. IEEE MTT-S Intl. Microwave Workshop on Wireless Sensing, Local Positioning, and RFID*, Cavtat, Croatia, Sept. 2009.
 [20] J. Searcy and S. Alland, "MIMO antenna with elevation detection," U.S. Patent 9 541 639 B2, Jan. 10, 2017.

[21] A. Moffet, "Minimum-redundancy linear arrays," *IEEE Trans. Antennas Propag.*, vol. 16, no. 2, pp. 172–175, 1968.
 [22] P. Pal and P. P. Vaidyanathan, "Nested arrays: A novel approach to array processing with enhanced degrees of freedom," *IEEE Trans. Signal Process.*, vol. 58, no. 8, pp. 4167–4181, 2010.
 [23] P. P. Vaidyanathan and P. Pal, "Sparse sensing with co-prime samplers and arrays," *IEEE Trans. Signal Process.*, vol. 59, no. 2, pp. 573–586, 2011.
 [24] S. Qin, Y. D. Zhang, and M. G. Amin, "Generalized coprime array configurations for direction-of-arrival estimation," *IEEE Trans. Signal Process.*, vol. 63, no. 6, pp. 1377–1390, 2015.
 [25] Z. Zheng, W. Wang, Y. Kong, and Y. D. Zhang, "Misc array: A new sparse array design achieving increased degrees of freedom and reduced mutual coupling effect," *IEEE Trans. Signal Process.*, vol. 67, no. 7, pp. 1728–1741, 2019.
 [26] P. Hacker and B. Yang, "Single snapshot DOA estimation," *Advances in Radio Science*, vol. 8, pp. 251–256, 2010.
 [27] S. Alland *et al.*, "Virtual radar configuration for 2D array," U.S. Patent 9 869 762, Jan. 16, 2018.
 [28] T. Spreng *et al.*, "Wideband 120 GHz to 140 GHz MIMO radar: System design and imaging results," in *Proc. European Microwave Conf. (EuMC)*, Paris, France, Sept. 2015.
 [29] Y. D. Zhang, M. G. Amin, F. Ahmad, and B. Himed, "DOA estimation using a sparse uniform linear array with two CW signals of co-prime frequencies," in *Proc. IEEE Intl. Workshop on Computational Advances in Multi-Sensor Adaptive Processing (CAMSAP)*, Saint Martin, Dec. 2013, pp. 404–407.
 [30] S. Qin, Y. D. Zhang, M. G. Amin, and B. Himed, "DOA estimation exploiting a uniform linear array with multiple co-prime frequencies," *Signal Process.*, vol. 130, pp. 37–46, 2017.
 [31] S. Zhang, A. Ahmed, Y. D. Zhang, and S. Sun, "DOA estimation exploiting interpolated multi-frequency sparse array," in *Proc. IEEE Sensor Array and Multichannel Signal Processing Workshop (SAM)*, Hangzhou, China, June 2020.
 [32] A. Ahmed, D. Silage, and Y. D. Zhang, "High-resolution target sensing using multi-frequency sparse array," in *Proc. IEEE Sensor Array and Multichannel Signal Processing Workshop (SAM)*, Hangzhou, China, June 2020.
 [33] Y. Yu, A. P. Petropulu, and H. V. Poor, "MIMO radar using compressive sampling," *IEEE J. Sel. Topics Signal Process.*, vol. 4, no. 1, pp. 146–163, 2010.
 [34] Y. Yu, S. Sun, R. N. Madan, and A. P. Petropulu, "Power allocation and waveform design for the compressive sensing based MIMO radar," *IEEE Trans. Aerosp. Electron. Syst.*, vol. 50, no. 2, pp. 898–909, 2014.
 [35] D. Chu, "Polyphase codes with good periodic correlation properties," *IEEE Trans. Inf. Theory*, vol. 18, no. 4, pp. 531–532, 1972.
 [36] R. T. Hoctor and S. A. Kassam, "The unifying role of the coarray in aperture synthesis for coherent and incoherent imaging," *Proc. IEEE*, vol. 78, no. 4, pp. 735–752, 1990.
 [37] C. Zhou, Y. Gu, X. Fan, Z. Shi, G. Mao, and Y. D. Zhang, "Direction-of-arrival estimation for coprime array via virtual array interpolation," *IEEE Trans. Signal Process.*, vol. 66, no. 22, pp. 5956–5971, 2018.
 [38] S. Sun and A. P. Petropulu, "A sparse linear array approach in automotive radars using matrix completion," in *Proc. IEEE Int. Conf. Acoust., Speech, Signal Process. (ICASSP)*, Barcelona, Spain, May 2020, pp. 8614–8618.
 [39] E. J. Candès and B. Recht, "Exact matrix completion via convex optimization," *Foundations of Computational Mathematics*, vol. 9, no. 6, pp. 717–772, 2009.
 [40] E. J. Candès and T. Tao, "The Dantzig selector: Statistical estimation when p is much larger than n ," *The Annals of Statistics*, vol. 35, no. 6, pp. 2313–2351, 2007.
 [41] T. T. Cai and L. Wang, "Orthogonal matching pursuit for sparse signal recovery with noise," *IEEE Trans. Inf. Theory*, vol. 57, no. 7, pp. 4680–4688, 2011.
 [42] E. J. Candès and J. Romberg, "Sparsity and incoherence in compressive sampling," *Inverse Problems*, vol. 23, pp. 969–985, 2007.
 [43] L. Carin, D. Liu, and B. Guo, "Coherence, compressive sensing, and random sensor arrays," *IEEE Antennas Propag. Mag.*, vol. 53, no. 4, pp. 28–39, 2011.